Supporting Information

Alkali metal partial substitution induced improved second-harmonic generation and enhanced laser-induced damage threshold for Ag-based sulfides

Wenfeng Zhou, Ming Geng, Mei Yan, Nian-Tzu Suen, Wenlong Liu, and Sheng-Ping Guo*

†School of Chemistry and Chemical Engineering, Yangzhou University, Yangzhou 225002, P. R. China

Corresponding author: spguo@yzu.edu.cn

Supplementary Information Index

Tables and Figures

Table S1. Crystal data and structure refinement parameters for **0**–**2**.

Chemical formula	**$Ag_2In_2GeS_6$** **(0)**	**$(LiAg)In_2GeS_6$** **(1)**	**$(NaAg)In_2GeS_6$** **(2)**
Fw	710.33	609.40	625.45
T/K		293(2)	
Crystal system		monoclinic	
Space group		*Cc*	
Z		4	
a/Å	12.2214(11)	12.1567(6)	12.0762(9)
b/Å	7.2156(7)	7.2525(4)	7.6256(5)
c/Å	12.2045(11)	12.1757(6)	12.1838(9)
β/°	109.567(2)	109.9070(10)	110.004(2)
V/Å^3	1014.10(16)	1009.34(9)	1054.29(13)
D_{calc} g/cm^3	4.653	4.010	3.940
μ/mm^{-1}	12.366	10.539	10.133
F(000)	1280.0	1104.0	1136.0
2θ range/°	6.664 to 51.98	6.654 to 51.994	6.438 to 51.986
Indep. Reflns/R_{int}	1938/0.0314	1919/0.0262	1887/0.0342
GOF on F^2	1.098	1.051	1.062
R1[a] [I ≥ 2σ (I)]	0.0188	0.0145	0.0226
wR2[b] [all data]	0.0421	0.0342	0.0577
Flack parameter	0.03 (2)	0.03 (2)	0.05 (3)

[a]$R1 = ||F_o| - |F_c||/|F_o|$. [b]$wR2 = [w(F_o^2 - F_c^2)^2]/[w(F_o^2)^2]^{1/2}$.

Table S2. Fractional atomic coordinates ($\times 10^4$) and equivalent isotropic displacement parameters ($Å^2 \times 10^3$) for **0**–**2**.

Atom	Wyckoff Gete	*x*	*y*	*z*	U_{eq}/Å^2
			0		
Ag(1)	4*a*	5032.6(7)	2102.8(12)	3482.4(8)	38.0(2)
Ag(2)	4*a*	3018.7(7)	5847.5(10)	1981.2(7)	34.1(2)
In(1)	4*a*	1415.0(5)	651.6(8)	1972.1(5)	14.21(16)
In(2)	4*a*	3239.1(5)	913.0(8)	8.7(5)	14.02(15)
Ge(1)	4*a*	762.6(7)	2368.6(11)	4420.8(7)	9.04(19)
S(1)	4*a*	3107.6(18)	2345(3)	1794.1(18)	15.0(4)
S(2)	4*a*	0.0(18)	33(3)	0.0(17)	15.4(4)
S(3)	4*a*	33.8(18)	2624(3)	2520.4(18)	14.7(4)
S(4)	4*a*	2658.0(19)	2424(3)	4920(2)	16.6(4)
S(5)	4*a*	6972.5(18)	2781(3)	3139.7(17)	14.2(4)
S(6)	4*a*	5268.4(17)	-151(3)	5205.9(17)	13.7(4)
			1		
Li(1)/Ag(1)	4*a*	5057.4(7)	2091.8(11)	3485.1(7)	39.3(2)
Li(2)/Ag(2)	4*a*	3004.5(18)	5848(2)	1967.6(18)	30.9(4)
In(1)	4*a*	1427.4(3)	673.0(5)	1969.0(3)	16.17(12)
In(2)	4*a*	3246.9(3)	902.0(6)	25.7(3)	16.51(12)
Ge(1)	4*a*	755.7(5)	2348.0(7)	4412.5(5)	10.53(14)
S(1)	4*a*	3119.3(14)	2383(2)	1793.8(14)	19.2(3)
S(2)	4*a*	1.9(13)	54(2)	-17.1(13)	17.6(3)
S(3)	4*a*	10.7(13)	2581(2)	2509.5(13)	17.6(3)
S(4)	4*a*	2663.8(14)	2411(2)	4952.5(15)	19.7(3)
S(5)	4*a*	6988.7(14)	2817(2)	3136.7(13)	18.5(3)
S(6)	4*a*	5285.9(12)	165(2)	200.6(12)	15.4(3)
			2		
Ag(1)	4*a*	5082.6(10)	2156.1(15)	3613.1(10)	45.1(3)

Na(1)	4*a*	2892(4)	5631(5)	1972(4)	21.1(9)
In(1)	4*a*	1406.1(5)	556.1(9)	1968.5(5)	16.36(19)
In(2)	4*a*	3274.5(5)	738.5(9)	47.2(5)	16.54(19)
Ge(1)	4*a*	775.5(9)	2353.6(12)	4370.6(9)	11.2(2)
S(1)	4*a*	3152(2)	2082(3)	1822(2)	20.1(5)
S(2)	4*a*	-6(2)	-104(3)	-24(2)	17.4(5)
S(3)	4*a*	23(2)	2521(3)	2464(2)	18.6(5)
S(4)	4*a*	2695(2)	2403(3)	4903(3)	20.8(5)
S(5)	4*a*	6977(2)	2937(3)	3211(2)	18.3(5)
S(6)	4*a*	5344(2)	239(3)	180(2)	15.2(5)

U_{eq} is defined as 1/3 of the trace of the orthogonanased U_{IJ} tensor.

Table S3. Bond lengths (Å) for **0**–**2**.

Bond	Length (Å)	Bond	Length (Å)
		0	
Ag(1)–S(1)	2.562(2)	In(1)–S(3)	2.466(2)
Ag(1)–S(2)#1	2.785(2)	In(1)–S(5)#5	2.477(2)
Ag(1)–S(5)	2.588(2)	In(2)–S(1)	2.465(2)
Ag(1)–S(6)	2.597(2)	In(2)–S(4)#6	2.503(2)
Ag(2)–S(1)	2.543(2)	In(2)–S(5)#7	2.474(2)
Ag(2)–S(3)#2	2.656(2)	In(2)–S(6)#6	2.472(2)
Ag(2)–S(4)#3	2.708(2)	Ge(1)–S(2)#8	2.193(2)
Ag(2)–S(5)#4	2.606(2)	Ge(1)–S(3)	2.196(2)
In(1)–S(1)	2.474(2)	Ge(1)–S(4)	2.189(2)
In(1)–S(2)	2.489(2)	Ge(1)–S(6)#4	2.208(2)
		1	
Li(1)Ag(1)–S(1)	2.556(2)	In(1)–S(3)	2.467 (2)
Li(1)Ag(1)–S(2)#1	2.775(2)	In(1)–S(5)#6	2.473 (2)
Li(1)Ag(1)–S(5)	2.578 (2)	In(2)–S(1)	2.458(2)
Li(1)Ag(1)–S(6)#2	2.593(2)	In(2)–S(4)#7	2.498(2)
Li(2)/Ag(2)–S(1)	2.530(2)	In(2)–S(5)#8	2.469 (2)
Li(2)/Ag(2)–S(3)#3	2.621(3)	In(2)–S(6)	2.473 (2)
Li(2)/Ag(2)–S(4)#4	2.663(3)	Ge(1)–S(2)#2	2.18 9(2)
Li(2)/Ag(2)–S(5)#5	2.605(3)	Ge(1)–S(3)	2.188(2)
In(1)–S(1)	2.472 (2)	Ge(1)–S(4)	2.186(2)
In(1)–S(2)	2.489 (2)	Ge(1)–S(6)#9	2.208(2)
		2	
Ag(1)–S(1)	2.593(3)	In(1)–S(3)	2.468(3)
Ag(1)–S(2)#1	2.818(3)	In(1)–S(5)#6	2.458(3)
Ag(1)–S(5)	2.568(3)	In(2)–S(1)	2.442(3)
Ag(1)–S(6)#2	2.582(3)	In(2)–S(4)#7	2.485(3)

Na(1)–S(1)	2.738(4)	In(2)–S(5)#8	2.466(3)
Na(1)–S(3)#3	2.829(5)	In(2)–S(6)	2.478(2)
Na(1)–S(4)#4	2.872(5)	Ge(1)–S(2)#2	2.203(2)
Na(1)–S(5)#5	2.781(5)	Ge(1)–S(3)	2.189(3)
Na(1)–S(6)#5	3.119(5)	Ge(1)–S(4)	2.183(3)
In(1)–S(1)	2.467(3)	Ge(1)–S(6)#9	2.228(2)
In(1)–S(2)	2.494(3)		

Symmetry codes: #1 1/2+*x*, 1/2-*y*, 1/2+*z*; #2 1/2+*x*, 1/2+*y*, +*z*; #3 +*x*, 1-*y*, -1/2+*z*; #4 -1/2+*x*, 1/2+*y*, +*z*; #5 -1/2+*x*, -1/2+*y*, +*z*; #6 +*x*, -*y*, -1/2+*z*; #7 -1/2+*x*, 1/2-*y*, -1/2+*z*; #8 +*x*, -*y*, 1/2+*z* for **1**; #1 1/2+*x*, 1/2-*y*, 1/2+*z*; #2 +*x*, -*y*, 1/2+*z*; #3 1/2+*x*, 1/2+*y*, +*z*; #4 +*x*, 1-*y*, -1/2+*z*; #5 -1/2+*x*, 1/2+*y*, +*z*; #6 -1/2+*x*, -1/2+*y*, +*z*; #7 +*x*, -*y*, -1/2+*z*; #8 -1/2+*x*, 1/2-*y*, -1/2+*z*; #9 -1/2+*x*, 1/2-*y*, 1/2+*z* for **2**; #1 1/2+*x*, 1/2-*y*, 1/2+*z*; #2 +*x*, -*y*, 1/2+*z*; #3 1/2+*x*, 1/2+*y*, +*z*;#4 +*x*, 1-*y*, -1/2+*z*;#5 -1/2+*x*, 1/2+*y*, +*z*; #6 -1/2+*x*, -1/2+*y*, +*z*; #7+*x*, -*y*, -1/2+*z*; #8-1/2+*x*, 1/2-*y*, -1/2+*z*; #9-1/2+*x*, 1/2-*y*, 1/2+*z* for **3**.

Table S4. The Ag/In molar ratios in **0**–**2** from EDS results.

Ag/In molar ratio	0	1	2
a	18.45/18.59 = 0.99	9.49/19.12 = 0.50	9.24/20.64 = 0.45
b	20.39/20.25 = 1.00	9.95/20.60 = 0.48	8.16/19.04 = 0.43

Note: a and b are the number of tests.

Table S5. The Ag/Na molar ratios in **2** from EDS results.

Ag/Na molar ratio	2
a	9.24/10.30 = 0.90
b	8.16/9.43 = 0.90

Note: a and b are the number of tests.

Table S6. Atomic coordinates and equivalent isotropic displacement parameters and the exact occupancies for Li/Ag in two co-occupation sites in **1**.

Compound	Atom	*x*	*y*	*z*	U_{eq}/Å^2	*Occupancy*
1	Li(1)	5057.4(7)	2091.8(11)	3485.1(7)	39.3(2)	0.25
	Ag(1)					0.75
	Li(2)	3004.5(18)	5848(2)	1967.6(18)	30.9(4)	0.75
	Ag(2)					0.25

Table S7. Atomic coordinates in calculation model for **1**.

Atom	*x*	*y*	*z*
Li(1)	0.11932	0.29082	0.40210
Ag(1)	0.11932	0.70918	0.90291
Ag(1)	0.61931	0.79082	0.40210
Ag(1)	0.61931	0.20918	0.90210
Li (2)	0.41403	0.41520	0.25035
Li (2)	0.41403	0.58480	0.75035
Li (2)	0.91403	0.08480	0.75035
Ag(2)	0.91403	0.91520	0.25035
In(1)	0.25613	0.93270	0.25049
In(1)	0.25613	0.06732	0.75049
In(1)	0.75631	0.43270	0.25049
In(1)	0.75631	0.56730	0.75049
In(2)	0.43826	0.90980	0.05616
In(2)	0.43826	0.09020	0.55616
In(2)	0.93826	0.40980	0.05616
In(2)	0.93826	0.59020	0.55616
Ge(1)	0.18914	0.23480	0.99485
Ge(1)	0.18914	0.76520	0.49485
Ge(1)	0.18914	0.23480	0.99485
Ge(1)	0.68914	0.73480	0.99485
Ge(1)	0.68914	0.26520	0.49485
Ge(1)	0.68914	0.73480	0.99485
S(1)	0.14216	0.48350	0.07365
S(1)	0.14216	0.51650	0.57365
S(1)	0.64216	0.98350	0.07365
S(1)	0.64216	0.01650	0.57365
S(2)	0.11464	0.74190	0.30454

S(2)	0.11464	0.25810	0.80454
S(2)	0.61464	0.24190	0.30454
S(2)	0.61464	0.75810	0.80454
S(3)	0.11376	0.99460	0.05189
S(3)	0.11376	0.00540	0.55189
S(3)	0.61376	0.49460	0.05189
S(3)	0.61376	0.50540	0.55189
S(4)	0.42550	0.76170	0.23298
S(4)	0.42550	0.23830	0.73298
S(4)	0.92550	0.26170	0.23298
S(4)	0.92550	0.73830	0.73298
S(5)	0.31244	0.21830	0.36726
S(5)	0.31244	0.78170	0.86726
S(5)	0.81244	0.71830	0.36726
S(5)	0.81244	0.28170	0.86726
S(6)	0.37996	0.24110	0.04885
S(6)	0.37996	0.75890	0.54885
S(6)	0.87996	0.74110	0.04885
S(6)	0.87996	0.25890	0.54885

Table S8. The NLO data of $A_2M^{III}{}_2M^{IV}Q_6$ (A = Li, Na; M^{III} = Ga, In; M^{IV} = Si, Ge, Sn) and $Na_2M^{II}M^{IV}{}_2Q_6$ (M^{II} = Zn, Cd, Hg; M^{IV} = Ge, Sn; Q = S, Se).

Compounds	Crystal system	Space group	Band gap (eV)	SHG	LIDTs	PM/NPM	Ref.
$Li_2Ga_2GeS_6$	Orthorhombic	*Fdd*2	3.65	1.2 × AGS	–	PM	[1]
$Li_2In_2SiS_6$	Monoclinic	*Cc*	3.61	1 × AGS	–	–	[2]
$Li_2In_2GeS_6$	Monoclinic	*Cc*	3.45	1 × AGS	–	–	[2]
$Li_2In_2SiSe_6$	Monoclinic	*Cc*	2.54	1 × AGSe	–	–	[2]
$Li_2In_2GeSe_6$	Monoclinic	*Cc*	2.30	1 × AGSe	–	–	[2]
$Na_2In_2SiS_6$	Monoclinic	*Cc*	2.47	0.3 × AGS	6.9 × AGS	PM	[3]
$Na_2In_2GeS_6$	Monoclinic	*Cc*	2.417	0.5 × AGS	4.0 × AGS	PM	[3]
$Na_2In_2GeSe_6$	Monoclinic	*Cc*	2.47	0.8 × AGS	–	–	[4]
$Na_2Ga_2GeS_6$	Orthorhombic	*Fdd*2	3.10	0.8 × AGS	18.1 × AGS	PM	[5]
$Na_2Ga_2SnS_6$	Orthorhombic	*Fdd*2	2.74	1.1 × AGS	18.0 × AGS	PM	[5]
$Na_2Ga_2GeSSe_5$	Orthorhombic	*Fdd*2	1.56	2.3 × AGS	9.9 × AGS	PM	[6]
$Na_2Ga_2GeSe_6$	Orthorhombic	*Fdd*2	1.61	1.6 × AGS	13.3 × AGS	PM	[6]
$Na_2Ga_2SnSSe_5$	Orthorhombic	*Fdd*2	1.63	3.9 × AGS	8.5 × AGS	PM	[6]
$Na_2Ga_2SnSe_6$	Orthorhombic	*Fdd*2	1.73	2.1 × AGS	10.1 × AGS	PM	[6]
$Na_2ZnGe_2S_6$	Monoclinic	*Cc*	3.25	0.9 × AGS	6 × AGS	PM	[7]
$Na_2ZnGe_2Se_6$	Tetragonal	*I4/mcm*	2.36	–	–	–	[4]
$Na_2ZnSn_2S_6$	Orthorhombic	*Fdd*2	2.71	4 × AGS	2 × AGS	NPM	[8]
$Na_2ZnSn_2Se_6$	Orthorhombic	*Fdd*2	2.05	3 × AGS	5 × AGS	PM	[9]
$Na_2CdGe_2S_6$	Monoclinic	*Cc*	3.21	0.8 × AGS	4.4 × AGS	PM	[10]
$Na_2CdGe_2Se_6$	Monoclinic	*Cc*	2.37	2 × AGS	–	PM	[10]
$Na_2CdSn_2Se_6$	Orthorhombic	*Fdd*2	2.15	2.2 × AGS	10 × AGS	PM	[9]
$Na_2HgSn_2Se_6$	Tetragonal	*I4/mcm*	1.83	–	–	–	[11]

Table S9. The SHG intensities of **0**–**2** in five different particle size ranges.

Compounds	25–45 μm (× AGS)	45–75 μm (× AGS)	75–110 μm (× AGS)	110–150 μm (× AGS)	150–210 μm (× AGS)	Average (× AGS)
0	0.4	0.4	0.4	0.4	0.5	0.42
1	0.9	0.8	0.8	0.9	0.8	0.84
2	1.3	1.2	1.2	1.2	1.2	1.22

Table S10. The statistical analysis of SHG intensities measurement for **0**–**2** and AGS.

Compounds	Particle sizes (μm)	SHG intensities (Volt)					
		1	**2**	**3**	**4**	**5**	**Average**
0	25–45	97.2	93.4	96	98	88.4	94.6
	45–75	126	126	124	126	128	126
	75–110	146	144	149	148	143	146
	110–150	186	186	196	184	188	188
	150–210	224	214	236	214	232	224
1	25–45	206	202	198	204	200	202
	45–75	292	284	288	290	286	288
	75–110	334	336	338	338	334	336
	110–150	392	396	395	398	399	396
	150–210	436	434	435	439	436	436
2	25–45	283	280	274	282	281	280
	45–75	414	408	412	408	418	412
	75–110	507	508	515	508	502	508
	110–150	574	574	570	576	566	572
	150–210	613	615	616	617	619	616
AGS	25–45	218	216	213	221	222	218
	45–75	351	340	339	353	337	344
	75–110	414	416	416	415	419	416
	110–150	456	453	460	462	469	460
	150–210	508	514	516	512	510	512

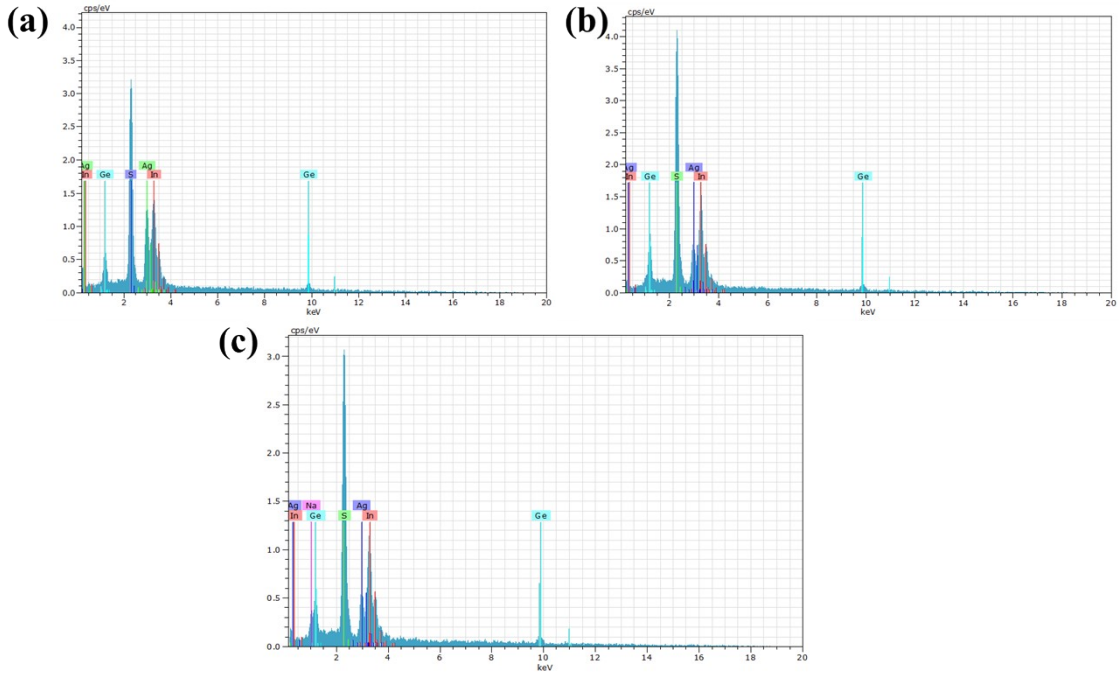

Fig. S1. The EDS images for single crystals of **0**–**2**.

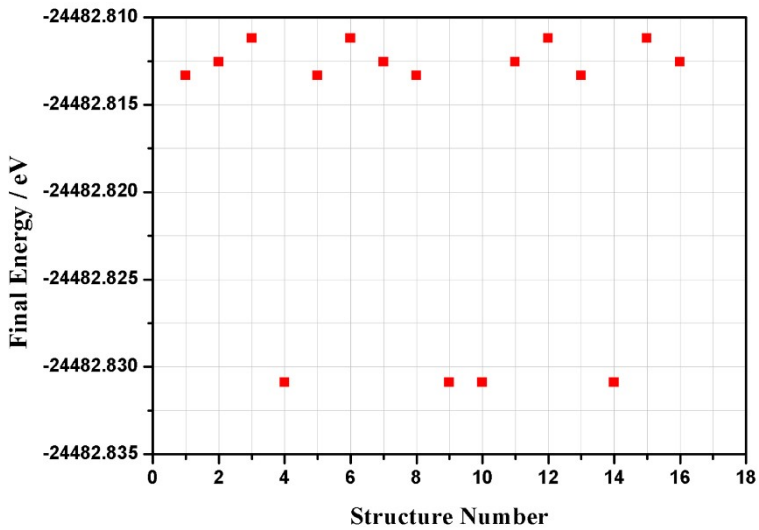

Fig. S2. A total 16 structure models of **1** in which 4 Ag and 4 Li atoms are randomly distributed over the eight Li/Ag sites.

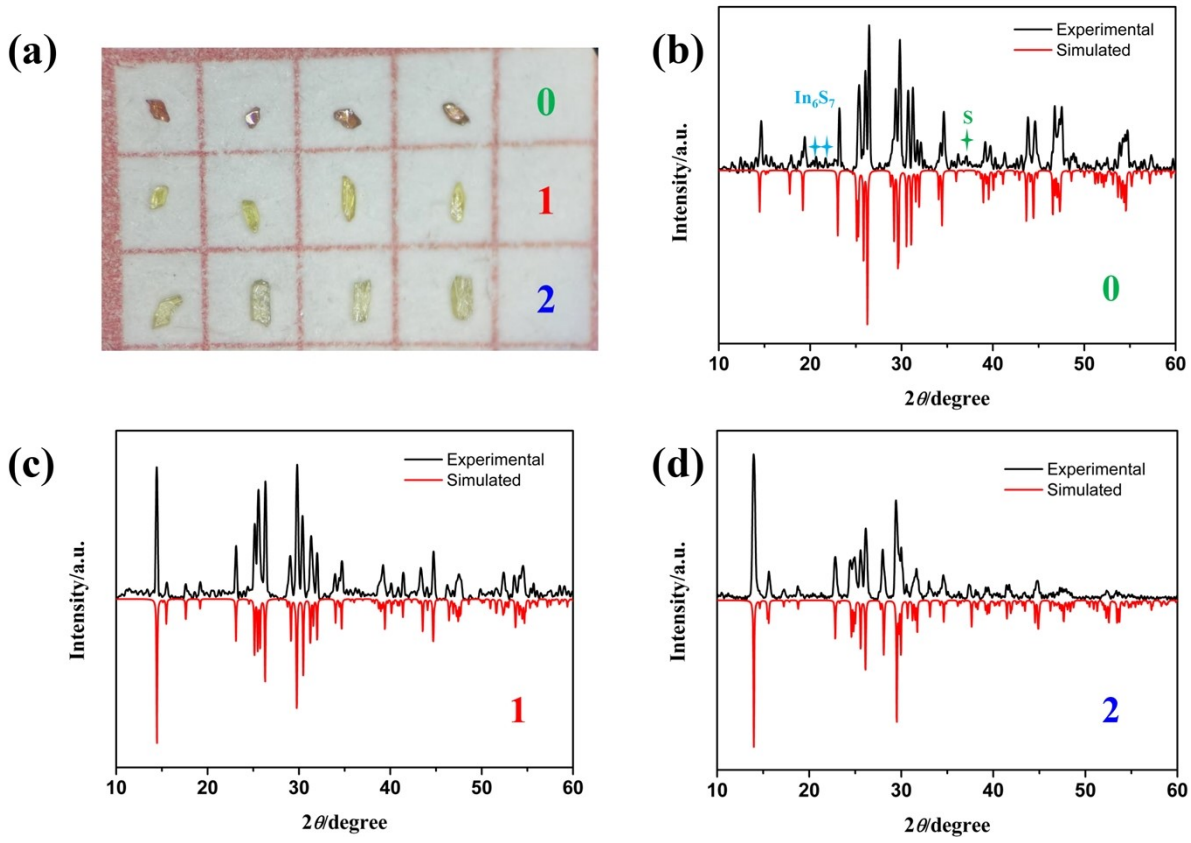

Fig. S3. (a) Photographs of the crystals for **0**–**2**. (b–d) Powder XRD patters for **0**–**2**.

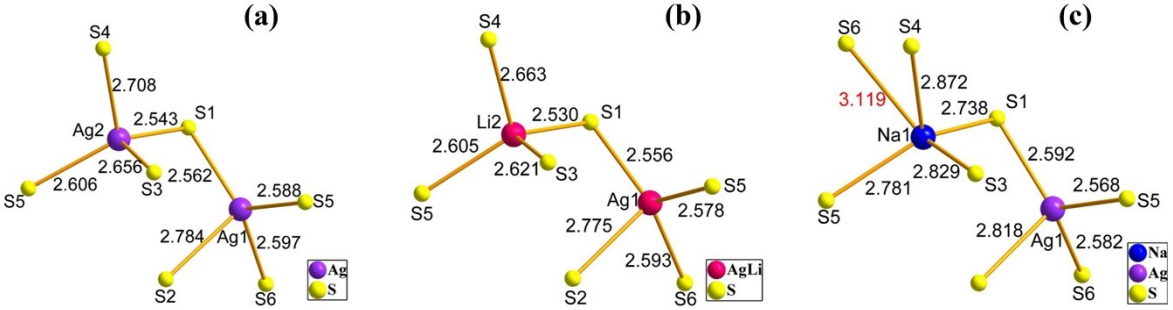

Fig. S4. Coordination environments of Ag, Ag/Li, and Na in **0**–**2**, respectively.

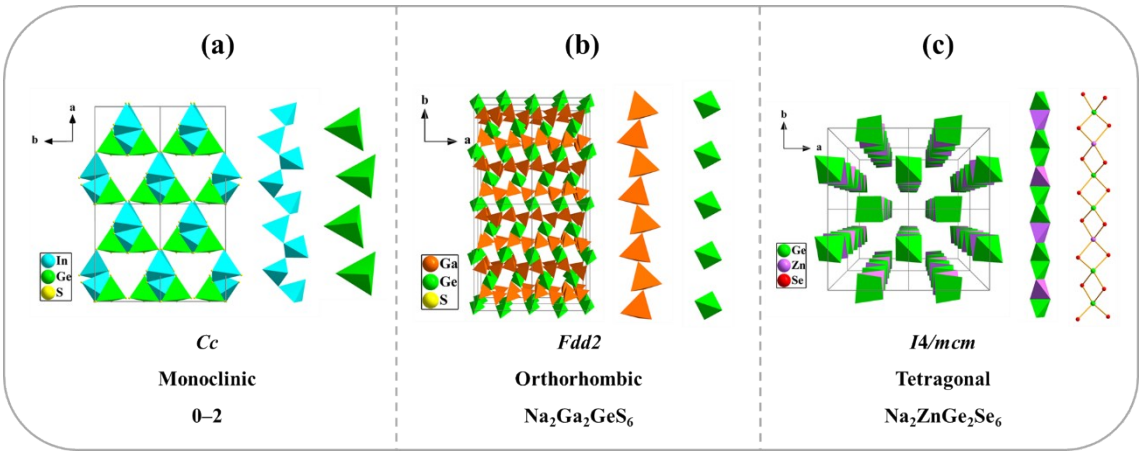

Fig. S5. Anion structural units in **0**–**2** (a), $Na_2Ga_2GeS_6$ (b), and $Na_2Zn_2GeSe_6$ (c).

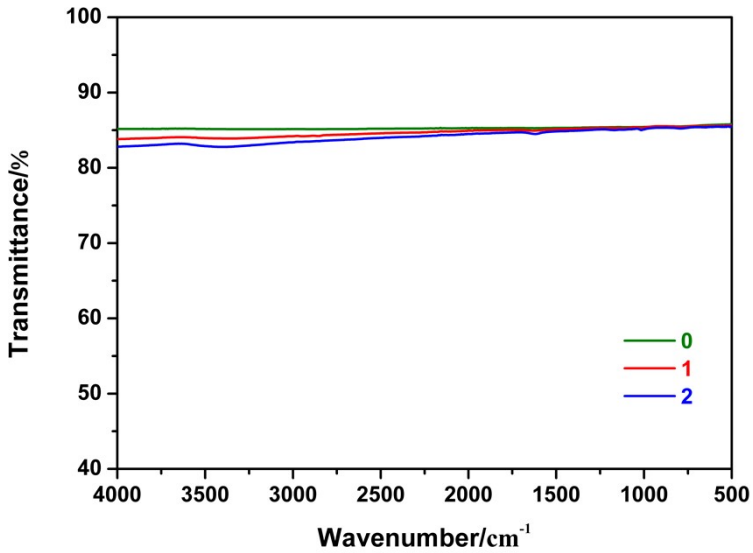

Fig. S6. FT-IR spectra of **0**–**2**.

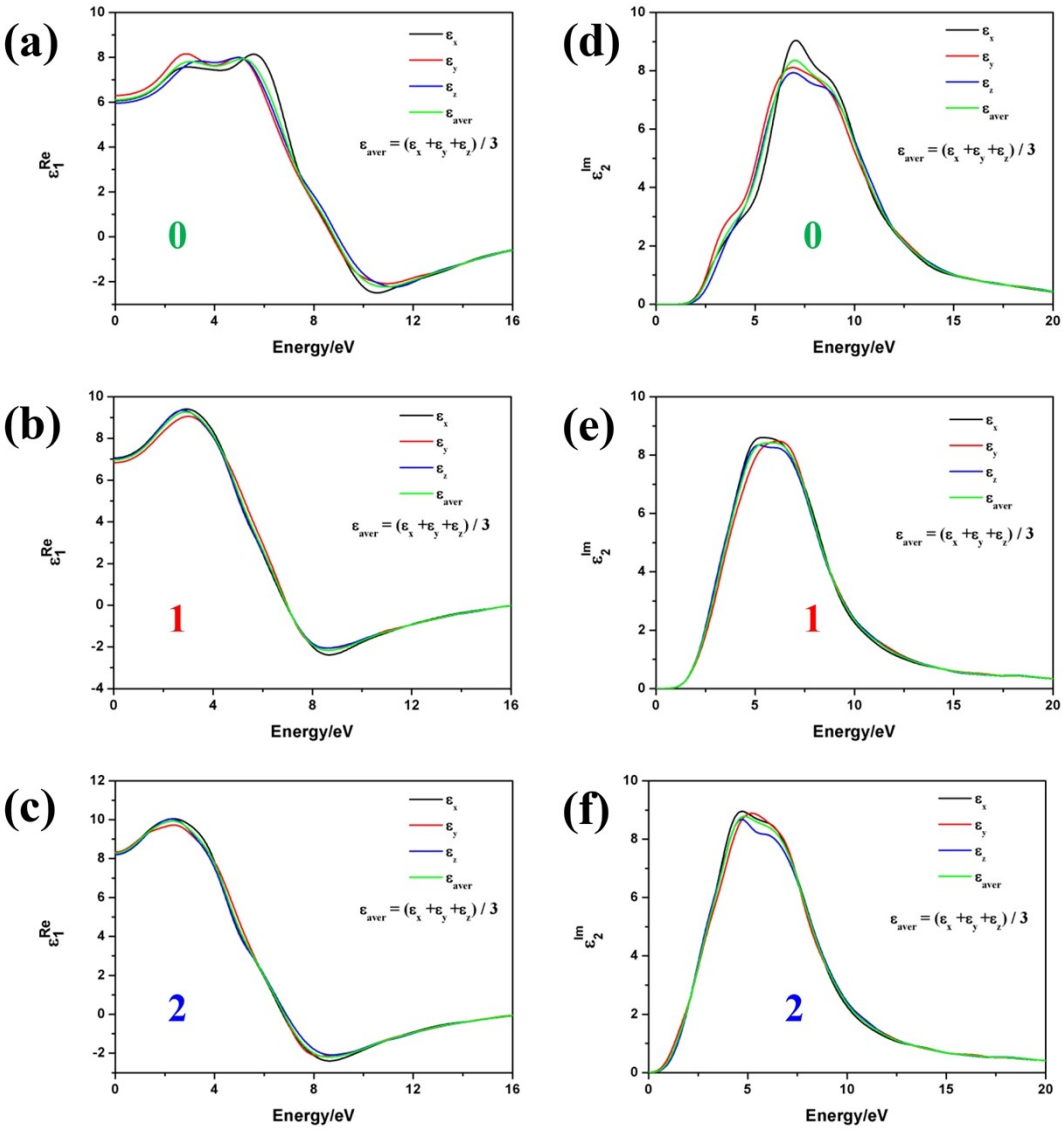

Fig. S7. The calculated real parts (a–c) and imaginary parts (d–f) of optical dielectric functions for **0**–**2**.

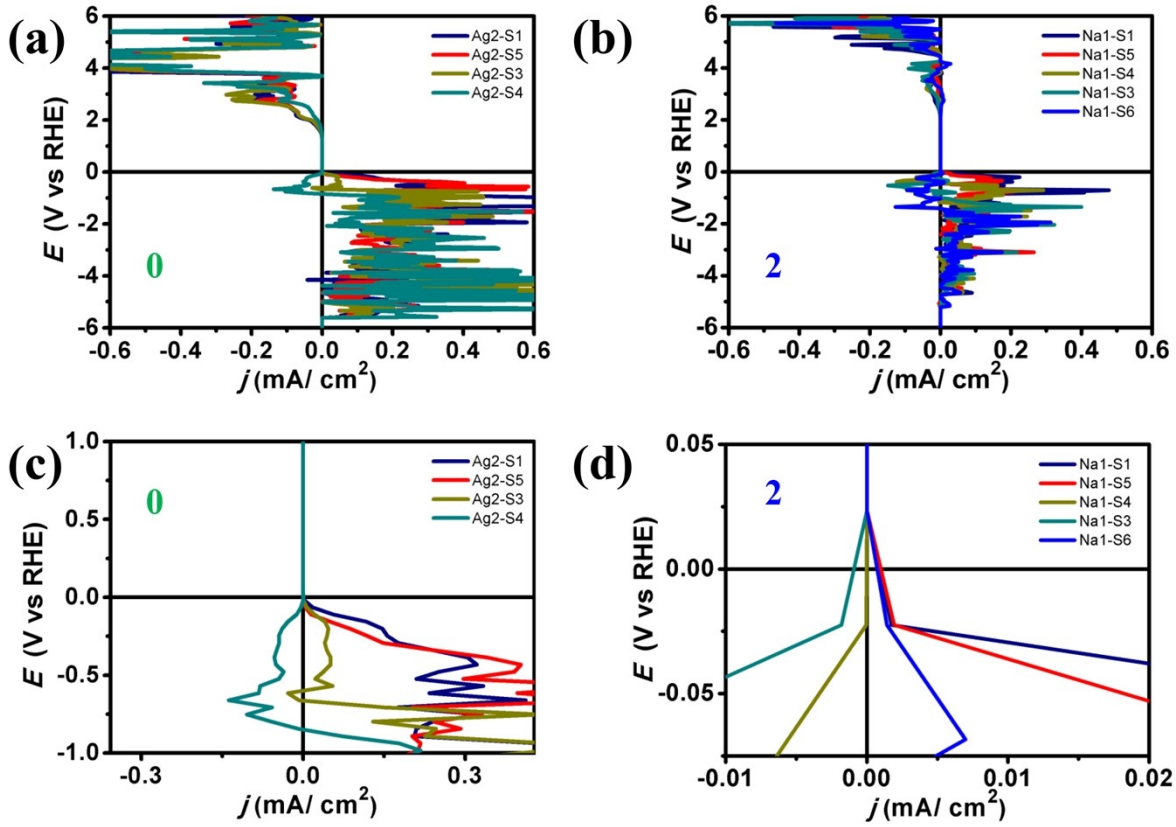

Fig. S8. Calculated COHP for **0** and **2**.

REFERENCES

1. Y. Kim, I. Seo, S. W. Martin, J. Baek, P. Shiv Halasyamani, N. Arumugam and H. Steinfink, Characterization of New Infrared Nonlinear Optical Material with High Laser Damage Threshold, $Li_2Ga_2GeS_6$, *Chem. Mater.*, 2008, **20**, 6048–6052.
2. W. L. Yin, K. Feng, W. Y. Hao, J. Y. Yao and Y. C. Wu, Synthesis, Structure, and Properties of $Li_2In_2MQ_6$ (M = Si, Ge; Q = S, Se): A New Series of IR Nonlinear Optical Materials, *Inorg. Chem.*, 2012, **51**, 5839–5843.
3. S. F. Li, B. W. Liu, M. J. Zhang, Y. H. Fan, H. Y. Zeng and G. C. Guo, Syntheses, Structures, and Nonlinear Optical Properties of Two Sulfides $Na_2In_2MS_6$ (M = Si, Ge), *Inorg. Chem.*, 2016, **55**, 1480–1485.
4. M. L. Zhou, C. Li, X. S. Li, J. Y. Yao and Y. C. Wu, $K_2Sn_2ZnSe_6$, $Na_2Ge_2ZnSe_6$, and $Na_2In_2GeSe_6$: A New Series of Quaternary Selenides with Intriguing Structural Diversity and Nonlinear Optical Properties, *Dalton Trans.*, 2016, **45**, 7627–7633.

5. S. F. Li, X. M. Jiang, B. W. Liu, D. Yan, H. Y. Zeng and G. C. Guo, Strong Infrared Nonlinear Optical Efficiency and High Laser Damage Threshold Realized in Quaternary Alkali Metal Sulfides $Na_2Ga_2MS_6$ (M = Ge, Sn) Containing Mixed Nonlinear Optically Active Motifs, *Inorg. Chem.*, 2018, **57**, 6783–6786.

6. S. F. Li, X. M. Jiang, Y. H. Fan, B. W. Liu, H. Y. Zeng and G. C. Guo, New Strategy for Designing Promising Mid-Infrared Nonlinear Optical Materials: Narrowing the Band Gap for Large Nonlinear Optical Efficiencies and Reducing the Thermal Effect for a High Laser-Induced Damage Threshold, *Chem. Sci.*, 2018, **9**, 5700–5708.

7. G. M. Li, K. Wu, Q. Z. Liu, Z. H. Yang and S. L. Pan, $Na_2ZnGe_2S_6$: A New Infrared Nonlinear Optical Material with Good Balance between Large Second-Harmonic Generation Response and High Laser Damage Threshold, *J. Am. Chem. Soc.*, 2016, **138**, 7422–7428.

8. G. M. Li, K. Wu, Q. Liu, Z. H. Yang and S. L. Pan, $Na_2ZnSn_2S_6$: A Mixed-Metal Thiostannate with Large Second-Harmonic Generation Response Activated by Penta-Tetrahedral $[ZnSn_4S_{14}]^{10-}$ Clusters, *Sci. China Technol. Sc.*, 2017, **60**, 1465–1472.

9. R. Ye, X. Y. Cheng, B. W. Liu, X. M. Jiang, L. Q. Yang, S. Q. Deng and G. C. Guo, Strong Nonlinear Optical Effect Attained by Atom-Response-Theory Aided Design in the $Na_2M^{II}M^{IV2}Q_6$ (M^{II} = Zn, Cd; M^{IV} = Ge, Sn; Q = S, Se) Chalcogenide System, *J. Mater. Chem. C*, 2020, **8**, 1244–1247.

10. G. M. Li, Q. Liu, K. Wu, Z. H. Yang and S. L. Pan, $Na_2CdGe_2Q_6$ (Q = S, Se): Two Metal-Mixed Chalcogenides with Phase-Matching Abilities and Large Second-Harmonic Generation Responses, *Dalton Trans.*, 2017, **46**, 2778–2784.

11. Z. Li, Y. Q. Liu, S. Z. Zhang, W. H. Xing, W. L. Yin, Z. S. Lin, J. Y. Yao and Y. C. Wu, Functional Chalcogenide $Na_2HgSn_2Se_6$ and $K_2MnGe_2Se_6$ Exhibiting Flexible Chain Structure and Intriguing Birefringence Tunability, *Inorg. Chem.*, 2020, **59**, 7614–7621.